Wall pressure fluctuations of turbulent separated and reattaching flow with local forcing

by

Y.Z. Liu [(1)], W. Kang[(2)] and H.J. Sung[(3)]

Department of Power Machinery Engineering

Shanghai Jiaotong University

Huashan Road 1954, Shanghai 200030; China

[(1)]E-mail: yzliu@sjtu.edu.cn

Department of Mechanical Engineering

Korea Advanced Institute of Science and Technology

373-1, Kuseong-dong Yuseong-gu, Daejeon, 305-701; Korea

[(2)]E-Mail: gracekang@kaist.ac.kr

Correspondence to [(3)]E-Mail: hjsung@kaist.ac.kr

ABSTRACT

Assessment of the organized turbulent separated and reattaching flow by local forcing was made by measuring wall pressure fluctuations. Multi-arrayed microphones as shown in Fig.1 were installed on the surface to measure the simultaneous spatial and temporal wall pressure fluctuations. The local forcing at the separation edge was given to the separated flow over a backward-facing step through a thin slit. The separated and reattaching flow was found to be most organized at the effective forcing frequency. The organized flow structure by local forcing was diagnosed by analyzing the information of wall pressure fluctuations. Several characteristics of wall pressure fluctuations were obtained: wall pressure fluctuation coefficients, wall pressure spectrum, wavenumber-frequency spectrum, coherence, cross-correlation, and multi-resolution autocorrelations of pressure fluctuations using the maximum overlap discrete wavelet transform (MODWT) and continuous wavelet transform (CWT). The amalgamation processes of vortices were observed, which gave the maximum reduction of the reattachment length. The enhancements of the flapping motion and streamwise dispersion of vortical structures were examined by the wall pressure fluctuations.

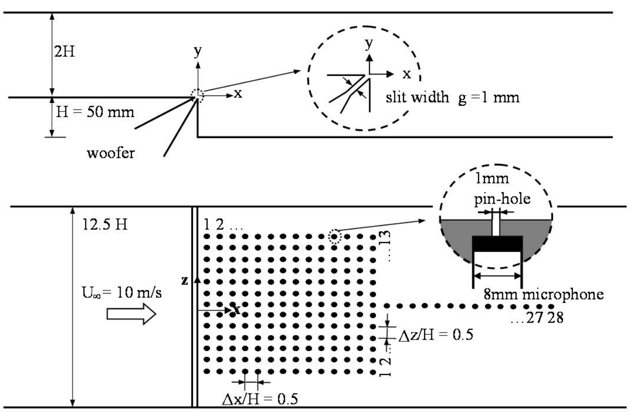

Fig. 1. Experimental setup of backward-facing step with a speaker and arrangement of multi-arrayed microphones

1. INTRODUCTION

A large number of attempts have been made to control turbulent separated and reattaching flows. Among others, the local forcing at the separation edge received much attention (Miau et al. 1991; Sigurdson 1995; Chun and Sung 1996; Kiya et al. 1997; Chun and Sung 1998; Yoshioka et al. 2001). The turbulent separated and reattaching flow over a backward-facing step was most organized by giving local forcing at the effective forcing frequency (Chun and Sung 1996). To assess the organized flow, extensive measurements were made, e.g., mean and turbulent velocity quantities, reattachment length and velocity spectra. Much time is needed to measure the whole flow structure. Alternatively, measurement of wall pressure fluctuations on the surface is a simple and efficient way to assess the organization of flow structures. This is because wall pressure fluctuations are closely related with vortical flow structures above the wall. Furthermore, wall pressure fluctuations are footprints of the convecting vortices over the wall (Kim et al. 2002).

A literature survey reveals that many studies of wall pressure fluctuations have been made to portray the unsteady behaviors of separated and reattching flows, e.g., flapping of reattaching shear layer and shedding of large-scale vortical structures. Kiya and Sasaki (1983) observed large-scale vortical structure in the reattaching zone using the cross-correlations between wall pressure fluctuations and velocity fluctuations. The large-scale vortical structure was educed by a conditional signal of wall pressure fluctuations (Kiya and Sasaki 1985). Farabee and Casella (1986) used one microphone to measure wall pressure spectrum of separated flows. However, multi-arrayed microphones were used to measure time-mean statistics (Lee and Sung 2001) and spatio-temporal characteristics (Lee and Sung 2002; Hudy et al. 2003). Recently, the interaction of unsteady wake and turbulent separated and reattaching flow over backward-facing step was examined using synchronized measurement of streamwise and spanwise wall pressure fluctuations (Chun et al. 2003). The conditional sampling in spatial domain with a spatial box filtering of wall pressure fluctiations was adopted to extract large-scale vortical structure under the influence of periodic wake (Lee and Sung 2002).

The main objective of the present study is to assess the flow organization by measuring wall pressure fluctuations. The separated and reattaching flow with local forcing was chosen in the present study (Chun and Sung 1996). This is because the turbulent separated and reattaching is well organized by imposing local forcing at the effective forcing frequency. Multi-arrayed microphones were installed in the bottom wall surface of the flow over a backward-facing step. The flow forcing condition was the same as that of Chun and Sung (1996). Synchronized measurements of wall pressure fluctuations in the streamwise direction were performed using multi-arrayed microphones. The wall pressure fluctuations with and without local forcing were compared. The flow organization was examined in terms of wall pressure spectrum, pressure fluctuation coefficients, auto- and cross-correlation, wavenumber-frequency spectrum. The temporal and spatial characteristics of vortical structures were analyzed using the maximum overlap discrete wavelet transform (MODWT) and continuous wavelet transform (CWT). At the effective forcing frequency, the promoted amalgamations of spanwise vortices were observed, which gave the maximumreduction of reattachment length.

2. EXPERIMENTAL APPARATUS and PROCEDURE

Experiments were performed in a subsonic open-circuit wind tunnel. Details regarding the experimental apparatus and the acoustic local forcing can be found in Chun and Sung (1996) and Lee and Sung (2002). Special attention was given to removing the tunnel floor vibration, which was transmitted from the forcing chamber with the installation of a woofer speaker. The characteristic length of the backward-facing step was defined as the step height H=50mm. The aspect ratio AR based on H was 12.5 to satisfy the two-dimensionality of the flow (Brederode and Bradshaw 1978). In the present study, the free-stream flow speed used was 10m/s, resulting in a Reynolds number of 33,000 based on the step height H.

16 ICP-type microphones (TMS060A, Soritel Inc., Korea) were used in the present study and installed on the bottom surface of the expanded duct as shown in Fig.1. The microphones were installed at uniform interval of 0.5H ($1.25 \leq x/H \geq 8.75$). Synchronized measurements of wall pressure fluctuations with 16 microphones in the streamwise direction were carried out. To increase the spatial resolution and frequency resolution of each microphone, a pinhole of diameter 1mm and an installation cavity of diameter 8mm were drilled concentrically on the bottom plate (Chun et al. 2003). A 16-channel differential amplifier (PCB 513, The Modal Shop Inc.) was used to provide excitation power for the microphone, as well as the amplification of the fluctuating voltage signals. Each microphone was calibrated against a 0.5 inch B&K 4133 microphone. To rule out the data scatter associated with the uncertainty of the microphone calibration procedure (Hudy et al. 2002), the wall pressure fluctuation coefficients and wall pressure spectrum along the streamwise direction were obtained by sequential measurements using one microphone. Simultaneous acquisition of wall pressure fluctuation signals from the 16 microphones was made using LabVIEW software and a 64-channel A/D board (NI6110,

National Instruments Inc.). 409,600 time series data were acquired for each microphone with the sampling frequency of 7812.5Hz.

The preliminary velocity measurements were completed using a constant-temperature anemometer (IFA 300). The forcing amplitude was calibrated using a single-wire probe (TSI 1260) with 5 mm tungsten wire. The sampling frequency was fixed at 5 kHz. A split-film probe (TSI 1288) was used to measure the reattachment length (x_R) defined as the point where the forward-flow time fraction (g_p) in the vicinity of the wall (y/H=0.01) is equal to g_p=0.5. To resolve the time-mean reattachment length, the sampling frequency was fixed at 200Hz, and a total of 60,000 velocity data was obtained, indicating around 1,500 flapping motions (St=0.025) were encompassed in measurement.

In the context of the present study, care was exercised to clarify the spatio-temporal characteristics of wall pressure fluctuations. Toward this end, three forcing frequencies, St_f=0, 0.275 and 1.5, were chosen for comparison. As shown in Fig.2, the reattachment length of the separated and reattaching flow was reduced from x_R/H=7.75 at St_f=0 to x_R/H=5.65 at St_f=0.275, and increased to x_R/H=8.02 at St_f=1.5. These results were consistent with that of Chun and Sung (1996). The forcing amplitude A_0 in Chun and Sung (1996) was defined as the momentum change between the unforced flow and the forced flow in the initial boundary layer. However, this definition is not applicable to the numerical simulation. A simple definition (v_{rms}/U_∞) is better for the numerical simulation, where v_{rms} is the root-mean-square of total velocity fluctuating at the slit edge (x/H=-0.01, y/H=0). It is found that the previous forcing amplitude A_0=0.03 corresponds to v_{rms}/U_∞=0.6. The analysis of wall pressure fluctuations in time, frequency and wavenumber domains was carried out in terms of wall pressure fluctuation coefficients, autospectrum, coherence, wavenumber-frequency spectrum, and both the maximum overlap discrete wavelet transform (MODWT) (Percival and Walden 2000) and continuous wavelet transform (CWT).

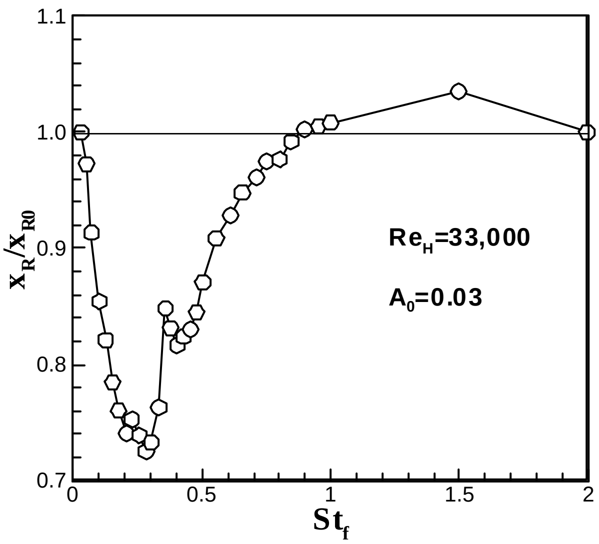

Fig.2 Reattachment variation dependent on forcing frequency at Re_H=33,000

3. EXPERIMENTAL RESULTS AND DISCUSSION

When the present local forcing experiment was performed, a severe speaker sound at higher forcing frequency was generated. This may give an influence on the microphones installed on the surface as a background noise. Prior to the main experiments of local forcing, influence of the background noise should be examined. Toward this end, the jet slit was blocked and no flow excitation was given through the thin slit. The wall pressure spectrum at x/H=7.75 was measured for three forcing frequencies St_f=0, 0.275 and 1.5 in Fig.3. Closer inspection of Fig.3 shows that very slight difference is detected at the lower frequency region (St $\leq$ 0.2). No significant effects of the background noise by speaker were shown for three forcing cases, although distinctive peaks were found at the forcing frequencies and their harmonics. As expected, the shedding of large-scale vortical structure and the flapping of reattaching shear layer were observed in the lower frequency region. This suggests that the influence of the background noise on the two main unsteady behaviors was negligible.

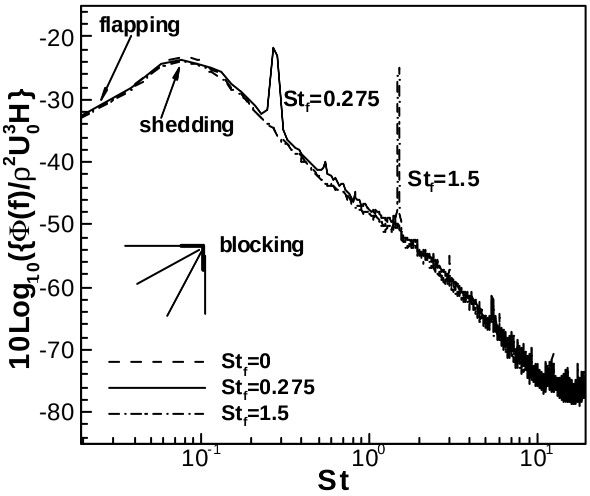

Fig.3 Wall-pressure spectrum influenced by background sound of speaker at x/H=7.75

To clarify the global characteristics of separated and reattaching shear layer, streamwise distributions of the rms pressure fluctuations $C_{p'}$ normalized by the inflow dynamic pressure q were displayed in Fig.4 (Lee and Sung 2001, 2002; Chun et al. 2003). For no forcing case (St_f =0), $C_{p'}$ increases along the streamwise direction in the range $0 \leq x/H \leq 7.25$, and then decreases ($x/H \geq 7.25$). The maximum $C_{p'}$ occurs slightly upstream of the time-mean reattachment point, which is in conformity with previous results of Lee and Sung (2001). When the forcing is applied at St_f=0.275, the position of the maximum $C_{p'}$ moves upstream by 2.5H. It is found that the $C_{p'}$ distribution at St_f=1.5 is almost similar to that of St_f=0. The correlation between x_R and $C_{p'}$ indicates that x_R can be predicted by $C_{p'}$, without direct measurement of x_R.

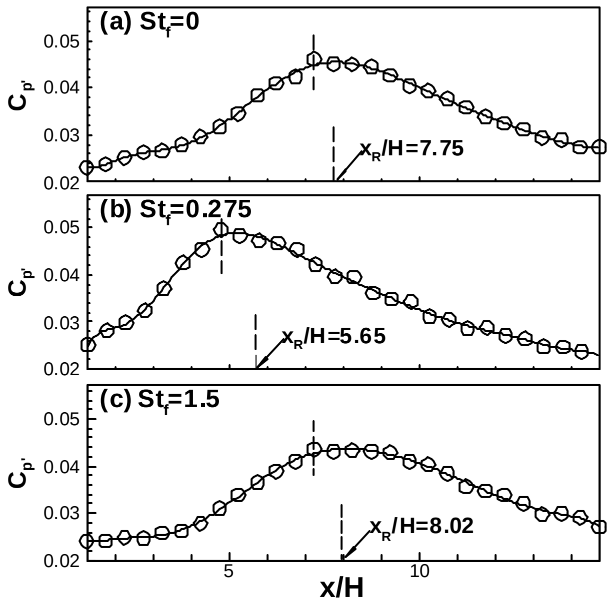

Fig.4 Wall-pressure fluctuation coefficient at Re_H=33,000

The influence of local forcing on the spatial development of vortical structure is obtained by measuring the wall pressure spectrum along the streamwise direction. Four positions are chosen in Fig.5; x/H=1.25, 4.25, 5.75 and 7.75. Near the separation edge at x/H=1.25, three characteristic frequencies are detected in Fig.5 (a), i.e., St=0.02, 0.07, and 0.13. The flapping frequency is present at St=0.02, where the normalized frequency fx_R/U_0=0.16 coincides with the value of Mabey (1972). The shedding frequency is at St=0.07, which is close to St=0.068 in Eaton (1980) and St=0.067 in Lee and Sung (2002). The merging frequency is detected at St=0.13, which is around twice the shedding frequency of large-scale vortical structure. When the local forcing is made at St_f=0.275, the flapping is significantly enhanced. It is found that the forcing at St_f=1.5 is not effective on wall pressure fluctuations. For both forcing cases (St_f=0.275 and 1.5), the higher frequency region is contaminated by the forcing frequencies and their harmonics. At x/H=4.25 shown in Fig.5 (b), a large upward shift of the spectrum is shown at St_f=0.275 and a slight downward shift is observed at St_f=1.5. The strengths of the flapping, shedding and merging frequencies are significantly enhanced due to the local forcing (St_f=0.275). The enhancement of flapping motion is closely related with the removal of corner flow by local forcing (Chun and Sung 1996). The merging frequency at St=0.13 appears to be strong as compared with other local forcings. This is manifest of the amalgamation of spanwise vortices. The promoted amalgamation process causes large entrainment close to the separation edge, which pushes the time-averaged streamlines downward the wall (Chun and Sung 1996). The slight downward shift of the spectrum at St_f=1.5 demonstrates that the quasi-deterministic coherent vortex structure is even attenuated at higher forcing frequency. As shown in Fig.5 (c), the intensity of shedding is enhanced for three cases. Recall that the reattachment length (x_R /H=5.65) at St_f=0.275 is close to the location (x/H=5.75). As the flow goes downstream, the vortical structure at St_f=0.275 starts to decay, while the vortical structure at St_f=0 begins to develop until reattachment (x/H=7.75). At x/H=7.75, comparison of the spectrum in Fig.5 (d) shows that the low frequency strength at St_f=0.275 is attenuated and even below that at St_f=0.

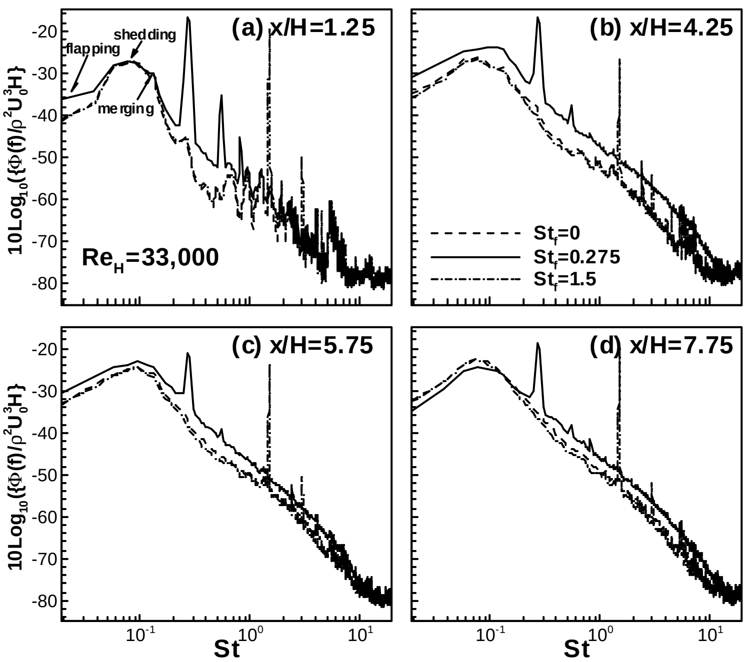

Fig.5 Wall-pressure spectrum at Re_H=33,000

(a) x/H=1.25 (b) x/H=5.25 (c) x/H=7.75 (d) x/H=10.25

Further comparison of the spatial strength variation of the vortical structure at the aforementioned shedding and merging frequencies is made for three forcing cases. Two prominent frequencies are chosen, St=0.07 and St=0.13; one is the shedding frequency and the other is the merging frequency. The wall pressure spectra at two fixed frequencies are replotted as a function of x/H in Fig.6. The spectrum of St=0.13 at St_f=0.275 rapidly increases near the separation edge until the maximum value is attained near x/H=4.25 and then quickly decays in the downstream direction. This indicates a fast process of the amalgamation of spanwise vortices. Recall that $C_{p'}$ near the separation edge rapidly increases at St_f =0.275. This is attributed to the dominance of the energetic shedding and merging motions. For St_f=0 and St_f=1.5, the strengths of St=0.13 slowly increase until the maximum is attained near x/H=5.75, and the flat plateaus centered at x/H=7.75 are formed. As mentioned earlier, the trend of wall pressure fluctuations of St_f=0 is almost similar to that of St_f =1.5, although the effect of St_f=0.275 is apparent. Accordingly, two forcing cases are chosen at St_f=0 and St_f=0.275 for further discussion.

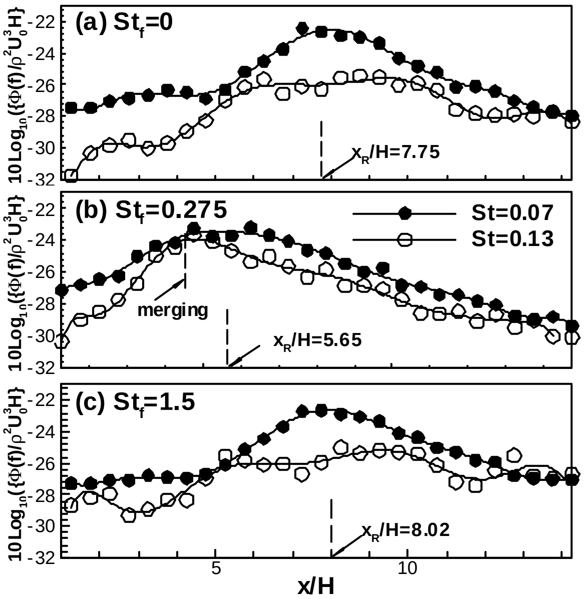

Fig.6 Spatial development of wall-pressure spectrum at St=0.07 and St=0.13

(a) St_f=0 (b) St_f=0.275 (c) St_f=1.5

In order to assess the flow structure organized by local forcing, we now consider the wall pressure fluctuations in terms of wavenumber-frequency spectra. The streamwise wavenumber-frequency spectrum $\Phi_{pp}(k_x, f; x_0)$ is obtained by Fourier transforming the streamwise cross spectrum $\Phi_{pp}(x, f; x_0)$ with respect to x. The spectra at the fixed frequencies *St*=0.02, 0.07 and 1.3 are illustrated in Fig.7 for comparison. The streamwise wavenumber-frequency spectrum exhibits two distinctive convective ridges near the separation edge (*x/H*=1.25), in good agreement with previous reports (Lee and Sung 2002; Hudy et al. 2003). These ridges, one slanted and the other horizontal along k_x =0, are signatures of shedding of the large-scale vortex and of flapping of the reattaching shear layer, respectively. From the slanted ridge, the convection velocity of the large-scale vortex was calculated as U_c / U_∞ =0.56. No clear difference is shown near the separation edge when the local forcing is introduced at St_f=0.275. However, when the reference point moves to *x/H*=4.25, the local forcing at St_f=0.275 globally increases the strength of the slanted ridge, and induces a discrete bubble-like area at *St*=0.13. This shows a strong amalgamation of the spanwise vortices. The frequency content of the convective ridge is enlarged up to high frequencies by local forcing. The dispersion of large-strength area along *St*=0.07 indicates an expansion of the influenced area by the large-scale vortical structures. Such dispersion of the vortical structure due to the local forcing is clear until *x/H*=5.75, but the extension of frequency contents of the convection ridge due to the local forcing is not attenuated even at *x/H*=7.75. However, no large difference of the dispersion along *St*=0.07 is demonstrated at *x/H*=7.75 for both forcing cases. For the shedding vortical structure at *St*=0.07, the strength at St_f=0.275 and *x/H*=5.75 is even weaker than strength at St_f=0 and *x/H*=7.75. This is consistent with the wall pressure spectrum in Figs.5 and 6.

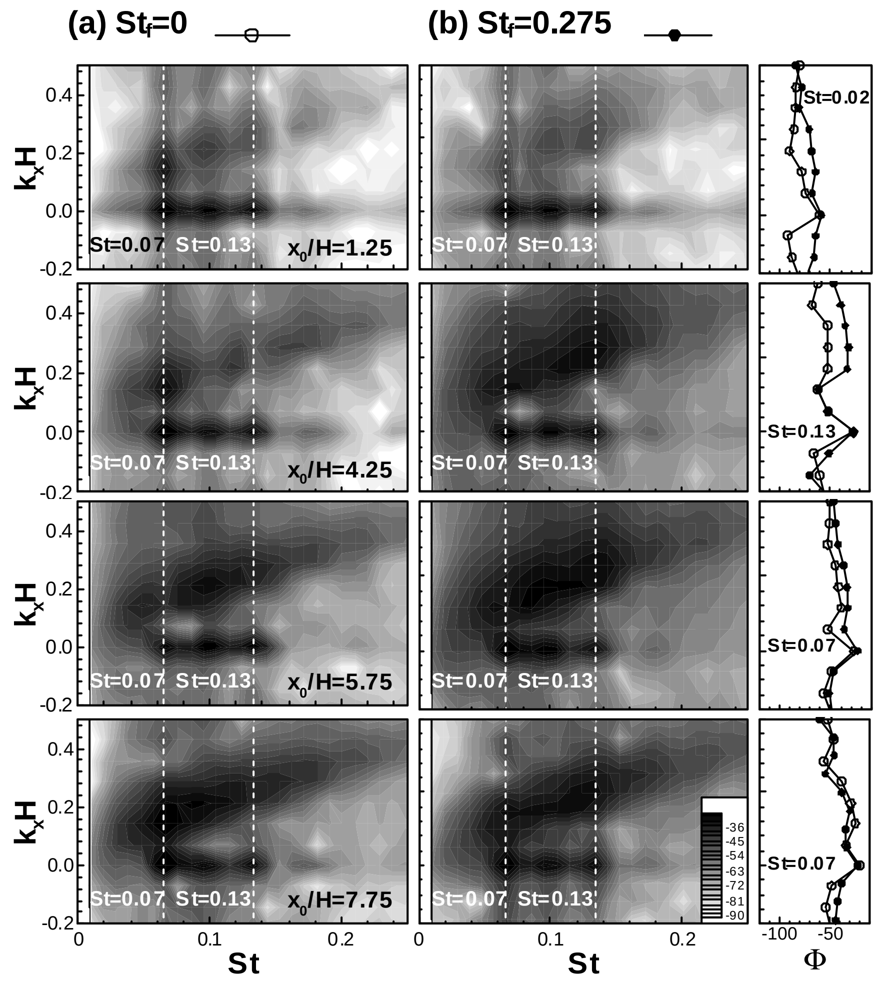

Fig.7 Streamwise wavenumber-frequency spectrum (a) St_f=0 and (b) St_f=0.275

Intermittent spatio-temporal behaviors of the amalgamation of spanwise vortices are scrutinized using the time-dependent analysis of these vortical structures. Using the maximum overlap discrete wavelet transform (MODWT), the multi-resolution autocorrelation of wall pressure fluctuations at *x/H*=4.25 is demonstrated in Fig.8. The multi-resolution autocorrelation is defined as

$$r_{pp}(x_0,\Delta t, f) =< p'_f(x_0,t)p'_f(x_0,t+\Delta t) > / < p'_f(x_0,t)p'_f(x_0,t) >, \tag{1}$$

where p'_f is reconstructed by inverse MODWT of the original pressure signals p' at the central frequency *f*. The direct autocorrelations of wall pressure fluctuations are displayed in Fig.8 for comparison. The direct autocorrelation is defined as

$$r_{pp}(x_0,\Delta t) =< p'(x_0,t)p'(x_0,t+\Delta t) > / < p'(x_0,t)p'(x_0,t) >. \tag{2}$$

Three unsteady behaviors are denoted using the dashed lines at St_f=0; flapping motion of the shear layer, shedding of large-scale vortical structures, and amalgamation of spanwise vortices. Close inspection of Fig.8 (a) reveals that another two merging processes exist at higher frequencies at *St* =0.26 and 0.52, which are harmonics of *St*=0.13. The amalgamation of spanwise vortices at *St*=0.13 is out-of-phase with the shedding of large-scale vortical structure at *St*=0.07. Another prominent vortical structure as denoted by the arrow at *St*=0.04 is out-of-phase with both the flapping motion of reattaching shear layer and the shedding of large-scale vortical structure. This may be a signature of the shedding of vortice, which is much larger than the regular vortices (*St*=0.07) near the reattaching point (Kiya and Sasaki 1983). When the local forcing is introduced at St_f=0.275, very clear ‘shutter-like’ distributions are shown at St=0.275 in Fig.8 (b). This forcing frequency overrides the first harmonic of *St*=0.13. As mentioned earlier, significant enhancement of the flapping motion is observed in Fig.5. In addition, a very large vortex at *St*=0.04 is enhanced, which results in the reduction of x_R but attenuates the successive shedding of regular vortice at St=0.07. The peaks of the direct autocorrelation curve at St_f=0 corresponds well to the shedding of large-scale vortical structures. However, these peaks are flattened at St_f=0.275 due to the aforementioned complex phase relations of the enhanced flapping motion at St=0.02 and the shedding of vortical structures at both St=0.04 and St=0.07.

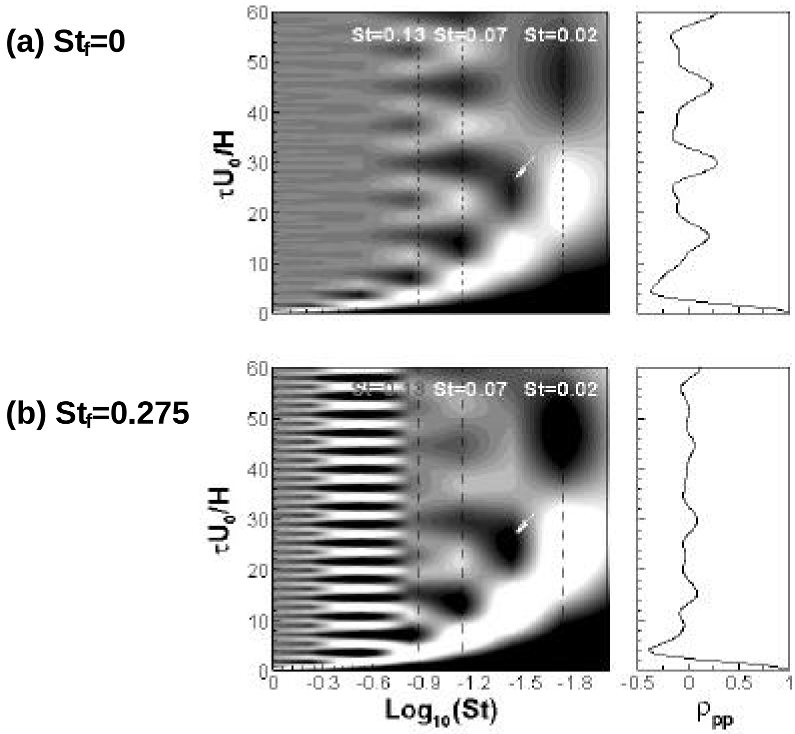

Fig.8 Auto-correlation of MODWT transformed wall pressure fluctuations at x/H=4.25

(a) St_f=0 and (b) St_f=0.275

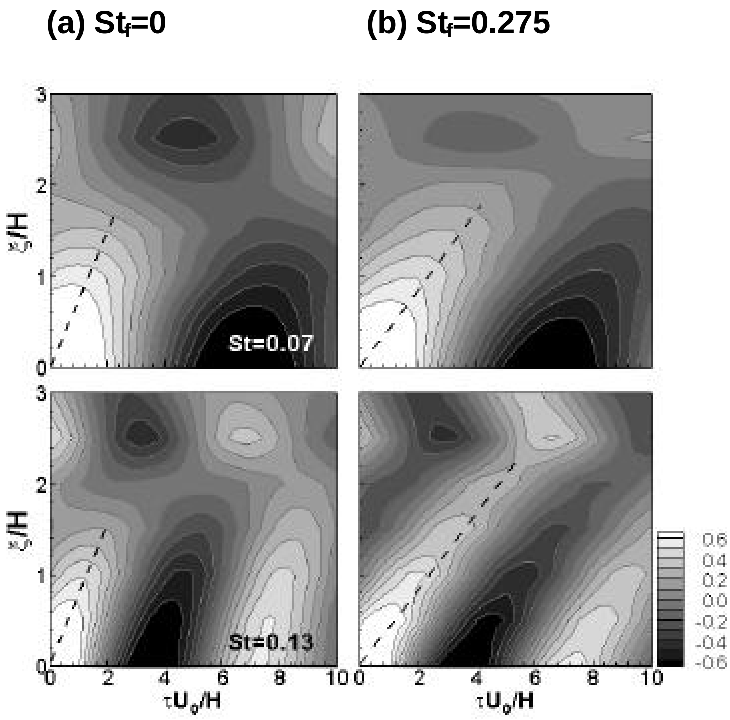

Fig.9 Streamwise cross-correlation of MOWDT transformed wall pressure fluctuations at

(a) St_f=0 and (b) St_f=0.275

By transforming the synchronized streamwise wall pressure fluctuations using the maximum overlap discrete wavelet transform (MODWT), the vortical structures centered at *St*=0.07 and *St*=0.13 are exemplified by cross-correlation of the extracted pressure signals. The cross-correlation is defined as

$$r_{pp}(x,\Delta t;x_0) = \langle p'_f(x_0,z_0,t)\,p'_f(x_0+x,t+\Delta t)\rangle / \langle p'_f(x_0,t)\,p'_f(x_0,t)\rangle . \qquad (3)$$

As shown in Fig.9, the large strength regions denoted by the dashed lines are extended downstream by local forcing. This is consistent with the enhanced dispersion of shedding and the amalgamation of spanwise vortices mentioned in Fig.7. Moreover, the convection velocities of both the regular large-scale vortical structure and the amalgamation of spanwise vortices are slightly decreased by the local forcing.

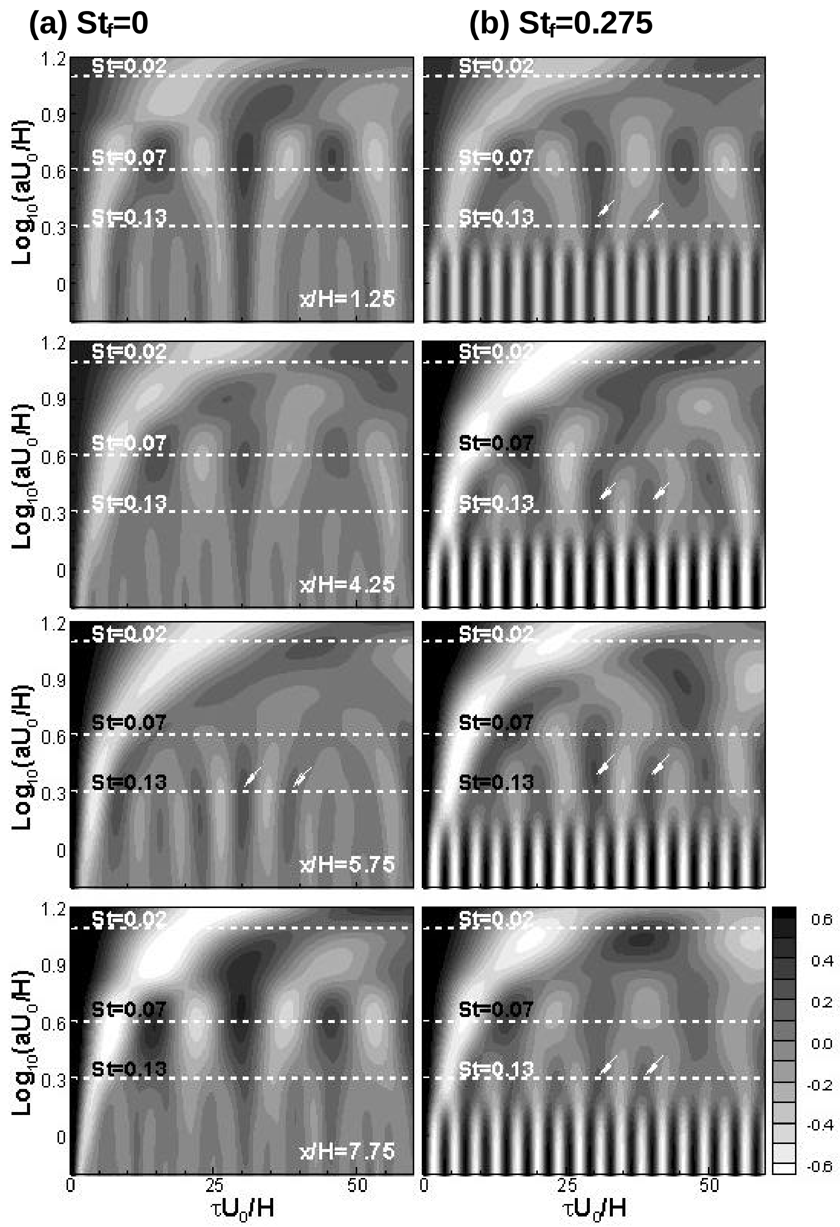

Fig.10 Auto-correlation of CWT coefficients of wall-pressure fluctuations at Re_H=33,000

(a) St_f=0 and (b) St_f=0.275

As discussed above, discrete wavelet transformation of the wall pressure fluctuations shows the intermittent scale-resolved vortical structures. However, the intermittent behaviors between *St*=0.13 and *St*=0.275 are not clearly detected due to the insufficient frequency resolution of discrete wavelet transformation, in which the central frequencies for each scale is approximated by half-band filters (Percival and Walden 2000). Toward this end, continuous wavelet transformation (CWT) of the wall pressure fluctuations is employed to extract the vortical structures at high frequency resolution. The continuous wavelet transform coefficient of a time-series data can be defined as

$$w(b,a) = \frac{1}{a}\int_{-\infty}^{+\infty} p(t)\Psi(\frac{t-b}{a})dt \,, \tag{4}$$

where a is the timescale dilation parameter and b is the time transition parameter. The relation between a and f is denoted by the conversion formula $f = \sqrt{2.5}/2pa$. The Mexican hat wavelet $\Psi(t) = (1-t^2)\exp(-\frac{1}{2}t^2)$ is used, which is known to be effective in resolving high amplitude peaks (Addision 1999; Poggie and Smits 1997). To clarify the intermittent vortical structures with high resolution, an analysis using the autocorrelation of CWT coefficients is then performed. The wavelet auto-correlation function $wc(\mathrm{a}, t)$ is defined as

$$wc(a,t) = < w(b,a)w(b+t,a) > / < w(b,a)wf(b,a) >, \tag{5}$$

where t is the time delay of wavelet coefficients in the wavelet space. Figure 10 shows the auto-correlation of CWT coefficients at St_f=0 and St_f=0.275. The main attention is given to the interaction between the amalgamation of spanwise vortices and the forcing frequency. Without forcing, the large strength areas denoted by arrows are observed at x/H=5.75, indicating the quasi-deterministic appearance of the amalgamation of spanwise vortices. However, these are not clear at the upstream positions (x/H=1.25, 4.25). For St_f =0.275, similar structures which are induced by two neighboring forcings at St=0.275 are clearly exemplified at x/H=4.25. The signatures of the strong amalgamations are still clear near the separation edge (x/H=1.25) and at the downstream positions (x/H=5.75, 7,75).

4. CONCLUSIONS

In the present study, measurements of wall pressure fluctuations were demonstrated to be an efficient method to delineate the organization of turbulent separated and reattaching flows. Measurements of wall pressure fluctuations using multi-arrayed microphones, not direct measurements of flow structure, were carried out to compare the flow structures for three forcing cases: St_f=0, 0.275 and 1.5. The influence of local forcing was systematically analyzed in terms of wall pressure fluctuation coefficients, wall pressure spectrum, cross-correlation, wavenumber-frequency spectrum and wavelet transforms. At St_f =0.275, the large upstream shift of wall pressure fluctuation coefficient was indicative of the reduction of the reattachment length. By local forcing, the streamwise dispersion of the vortical structures at St=0.07 (the shedding of large-scale vortical structures) and St=0.13 (the amalgamation of spanwise vortices) was demonstrated to be increased. The amalgamation of spanwise vortices at St_f=0.275 was clarified by wall pressure spectrum, multi-resolution auto-correlation of wall pressure fluctuations using the maximum overlap discrete wavelet transform (MODWT) and continuous wavelet transform (CWT). The intermittent amalgamation of spanwise vortices at St=0.13 gave the reduction of the reattachment length. The additional enhancement of flapping motion by local forcing was exemplified by showing the maximum overlap discrete wavelet transform (MODWT).

REFERENCES

Brederode, V. and Bradshaw, P. (1978). “Influence of the side walls on the turbulent center-plane boundary-layer in a square duct”, J Fluid Eng, 100, pp.91-96

Chun, K.B. and Sung, H.J. (1996). “Control of turbulent separated flow over a backward-facing step by local forcing”, Exp Fluids, 21, pp. 417-426

Chun, K.B. and Sung, H.J. (1998). “Visualization of Locally-Forced Separated Flow over a backward-facing Step”, Exp Fluids, 25, pp. 133-142

Chun, S., LIU, Y.Z. and Sung, H.J. (2003). “Wall pressure fluctuations of a turbulent separated and reattaching flow affected by an unsteady wake”, Exp Fluids (submitted)

Eaton, J.K. and Johnston, J.P. (1981), “A review of research on subsonic turbulent flow reattachment”, AIAA J, 19, pp. 1093-1100

Farabee, T.M. and Casarella, M.J. (1986). “Measurements of fluctuating wall pressure for separated/reattached boundary layer flows”, J Vib Acoust Stress Reliability Design, 108, pp. 301-307

Hudy, L.M., Naguib, A.M. and Humphreys, W.M. (2003). “Wall pressure-array measurements beneath a separating/reattaching flow region”, Phys. Fluids, 15, pp. 706-717

Kim, J., Choi, J.I. and Sung, H.J. (2002). “Relationship between wall pressure fluctuations and streamwise vortices in a turbulent boundary layer”, Phys. Fluids, 14, pp. 898-901

Kiya, M. and Sasaki, K. (1983). “Structure of a turbulent separation bubble”, J.Fluid Mech., 137,pp.83-113

Kiya, M. and Sasaki, K. (1985). “Structure of large-scale vortices and unsteady reverse flow in the reattaching zone of a turbulent separation bubble”, J Fluid Mech, 154, pp. 463-491

Kobashi, Y. (1986). “Wall pressure and its relation to turbulent structure of a boundary layer”, Experiments in fluids, 4, pp. 49-5

Lee, I. and Sung, H.J. (2002). “Multiple-arrayed pressure measurement for investigation of the unsteady flow structure of a reattaching shear layer”, J Fluid Mech, 463, pp. 377-402

Lee, I., Ahn, S.K. and Sung, H.J. (2004). “Three-Dimensional Coherent Structure in a Separated and Reattaching Flow over a Backward-Facing Step”, Exp. Fluids, (In press)

Li, H. (1998). “Identification of coherence structure in turbulent shear flow with wavelet correlation analysis”, J. Fluid Eng., 120, pp.778-785

Miau, J.J., Lee, K.C., Chen, M.H. and Chou, K.C. (1991). “Control of separated flow by a two-dimensional oscillatory plate”, AIAA J, 29, pp. 1140-1148

Percival, D.B. and Walden, A.T. (2000). “Wavelet methods for time series analysis”, Cambridge University Press

Sigurdson, L.W. (1995). “The structure and control of a turbulent reattaching flow”, J Fluid Mech, 298, pp. 139-165.

Yoshioka, S., Obi, S. and Masuda, S. (2001). “Turbulence statistics of periodically perturbed separated flow over a backward-facing step”, Int.J Heat and Fluid Flow, 22, pp. 393-401

Yoshioka, S., Obi, S. and Masuda, S. (2001). “Organized vortex motion in periodically perturbed turbulent separated flow over a backward-facing step”, Int.J Heat and Fluid Flow, 22, pp. 301-307